Spin and orbital angular momentum and their conversion in cylindrical vector vortices

Jiangbo Zhu,[1,2] Yujie Chen,[3] Yanfeng Zhang,[3] Xinlun Cai,[3,*] and Siyuan Yu[2,3,*]

[1]*State Key Lab of ASIC & System, Fudan University, Shanghai 200433, China*
[2]*Photonics Group, Merchant Venturers School of Engineering, University of Bristol, Bristol BS8 1UB, UK.*
[3]*State Key Laboratory of Optoelectronic Materials and Technologies, School of Physics and Engineering, Sun Yat-sen University, Guangzhou 510275, China.*
**Corresponding authors: caixinlun@gmail.com, s.yu@bristol.ac.uk*

Received Month X, XXXX; revised Month X, XXXX; accepted Month X, XXXX; posted Month X, XXXX (Doc. ID XXXXX); published Month X, XXXX

Generation of light beams carrying orbital angular momentum has been greatly advanced with the emergence of the recently reported integrated optical vortex emitters. Generally, optical vortices emitted by these devices possess cylindrically symmetric states of polarization and spiral phase fronts, and can be defined as cylindrical vector vortices. Using the radiation of angularly arranged dipoles to model the cylindrical vector vortices, these beams as hybrid modes of two circularly polarized scalar vortices are theoretically demonstrated to own well-defined total angular momentum. Moreover, the effect of spin-orbit interactions of angular momentum is identified in the cylindrical vector vortices when the size of the emitting structure varies. This effect results in the diminishing spin component of angular momentum, and the purer orbital angular momentum states at large structure radii.

OCIS Codes: (050.1940) Diffraction; (050.4865) Optical vortices; (260.5430) Polarization.

Recently, several novel integrated photonic devices have been proposed for the generation of optical vortex beams that carry photonic orbital angular momentum (OAM) [1-3], aiming at revolutionizing the research and application of OAM optics by enabling compact, robust and complex photonic integrated circuits that incorporate arrays of such devices. The optical vortex beams emitted by these integrated devices are vectorial in nature, often with cylindrical symmetry in their state-of-polarization (SOP) hence generalized as cylindrical vector vortices (CVVs).

In scalar optical vortices with a homogeneous SOP, such as linearly polarized Lagurre-Gaussian (LG) beams, it is well understood that the OAM per photon is well-defined as $\ell\hbar$ in the paraxial limit [4]. The classical manifestation of photonic OAM is in the form of a helical phase front resulting from the azimuthal varying phase term $\exp(j\ell\varphi)$, where ℓ is the topological charge and φ is the azimuthal angle. On the other hand, in CVVs, as it is the rotating vector field components that have the OAM-indicating phase dependence of $\exp(j\ell\varphi)$ [5], the phase evolution around the optical axis is accompanied by the SOP evolution. It has been suggested in [6, 7] that the vector elegant LG modes, with a similar spatial dependence of SOP and phase structure, possess the well-defined OAM states. However, the CVVs generated by these devices, as the hybrid modes of circularly polarized Bessel-like vortices [5], still imply an ambiguity in the total angular momentum (TAM), OAM, and SAM values. For many potential applications involving the use of OAM, either exploiting momentum transfer via light-matter interaction or using the OAM states to carry information, it is fundamentally important to clarify such ambiguity by quantifying the angular momentum and its constituents carried by the CVVs.

In this letter, we thoroughly investigate the TAM and its spin and orbital components carried by such CVVs using a classical approach. The TAM per photon of the emitted CVVs are found as well-defined by the topological charge as $\ell\hbar$ within the paraxial limit. On the other hand, the spin component per photon, which can be regarded as the contribution from the scalar vortex constituents carrying spin eigenstates of photon ($\pm\hbar$, respectively), is generally nonzero for all orders of topological charge. Furthermore, the spin-to-orbit conversion of angular momentum in CVVs is revealed when the size of the emitter varies.

In general, the OAM-carrying helical phase front of the CVVs emitted by the previously mentioned devices results from the local manipulation of phase or polarization of the input light by a number (q) of scattering/diffracting elements arranged in a circular fashion, characterized by a phase increment of $2\pi\ell/q$ between adjacent elements. Furthermore, these structures are fed by input optical modes with cylindrical symmetry. Therefore, all aforementioned CVV emitters can be represented by the composition of a common structure as shown in Fig. 1, i.e., a group of angular-distributed dipoles. The dipole elements in such groups have the SOPs arranged in a cylindrically symmetric fashion (either radially or azimuthally) and the initial phase states defined by the topological charge as $\{\phi_m = 2\pi\ell m/q\}$, where $m = 1, 2, \ldots, q$. Hence the CVV emitters can all be analyzed using the theoretical model developed in [5]. All dipoles $\{\mathbf{P}_m^A\}$ are assumed with a uniform moment of P_A, a time dependence of $\exp(-j\omega t)$, and located evenly along the circumference with $\rho = 1$ on the emitter plane ($\zeta = 0$), where (ρ, φ, ζ) is the dimensionless cylindrical coordinates, with $\rho = r/R$ and $\zeta = z/R$ as the polar radius and vertical distance normalized to the radius of the dipole group, R.

The case of azimuthally polarized angular dipoles (APADs) is considered first. Under the paraxial limit and in the far-field zone of dipole radiation ($\zeta \gg \lambda/R$), the cylindrical components of the emitted beam are [5]

$$E^A_{\rho,\ell} = (-j)^{\ell}\frac{\mathrm{A}\nu^2\Phi(\rho,\zeta)}{\sqrt{\rho^2+\zeta^2}}\exp(j\ell\varphi)(J_{\ell+1}+J_{\ell-1}) \quad (1a)$$

$$E^A_{\varphi,\ell} = (-j)^{\ell+1}\frac{\mathrm{A}\nu^2\Phi(\rho,\zeta)}{\sqrt{\rho^2+\zeta^2}}\exp(j\ell\varphi)(J_{\ell+1}-J_{\ell-1}) \quad (1b)$$

$$E^A_{\zeta,\ell} = -(-j)^{\ell}\frac{\mathrm{A}\nu^2\rho\zeta\Phi(\rho,\zeta)}{(\rho^2+\zeta^2)^{3/2}}\exp(j\ell\varphi)(J_{\ell+1}+J_{\ell-1}) \quad (1c)$$

where the constant $\mathrm{A} = \mathrm{P}_A q/8\pi\varepsilon_0 R^3$, the normalized propagation constant $\nu = 2\pi R/\lambda$ (λ as the vacuum wavelength), the propagation phase factor $\Phi(\rho,\zeta) = \exp[j\nu(2\zeta^2+\rho^2+1)/2\zeta]$, and $J_i \equiv J_i(\nu\rho/\zeta)$ denotes the i^{th} order Bessel function of the first kind.

The Jones vector of the transverse field of the APADs emitted CVV can be written from Eq. (1a) and (1b) as

$$\mathbf{E}^A_{T,\ell} = \begin{bmatrix} E^A_{x,\ell} & E^A_{y,\ell}\end{bmatrix}^T = (-j)^{\ell}\frac{\mathrm{A}\nu^2\Phi(\rho,\zeta)}{\sqrt{\rho^2+\zeta^2}} \times\left\{J_{\ell-1}e^{j(\ell-1)\varphi}\begin{bmatrix}1 & j\end{bmatrix}^T + J_{\ell+1}e^{j(\ell+1)\varphi}\begin{bmatrix}1 & -j\end{bmatrix}^T\right\} \quad (2)$$

Accordingly, normalized Stokes parameters in the circular polarization basis at the point (ρ, φ, ζ) can be obtained as

$$S^A_{1,\ell} = 2J_{\ell-1}J_{\ell+1}\cos 2\varphi\Big/\left(J^2_{\ell-1}+J^2_{\ell+1}\right) \quad (3a)$$

$$S^A_{2,\ell} = 2J_{\ell-1}J_{\ell+1}\sin 2\varphi\Big/\left(J^2_{\ell-1}+J^2_{\ell+1}\right) \quad (3b)$$

$$S^A_{3,\ell} = \left(J^2_{\ell-1}-J^2_{\ell+1}\right)\Big/\left(J^2_{\ell-1}+J^2_{\ell+1}\right) \quad (3c)$$

Note that the SOP of the CVV is not globally defined, but distributed in a pattern cylindrically symmetric with respect to the propagating axis, and dependent on the local values of both functions $J_{\ell+1}$ and $J_{\ell-1}$. Moreover, Eqs. (1a)-(1c) indicate that the cylindrical vector components have the common azimuthal phase dependence of $\exp(j\ell\varphi)$, suggesting the vectorial vortex nature of the beams emitted by these devices. This feature, along with the circularly polarized vortices separation presented in Eq. (2), is also shared by the exact LG vector beams and the quasi-nondiffracting Bessel light beams [6, 8]. However, the exact OAM quantity carried by such CVVs still requires careful examination, as the circularly polarized vortex components in Eq. (2) are not typical eigenmodes of the wave function.

The ζ components of the SAM and OAM per photon per unit length for the paraxial beams in Eq. (2) can be calculated by, for example, Eq. (8) in [9]. It should be noted that Eqs. (1a)-(1c) and (2) have been modified into a more precise form ($\propto 1/(\rho^2+\zeta^2)^{1/2}$), compared with those in [5] ($\propto 1/\zeta$). The transverse components thus vanish sufficiently fast to result in a convergent integral across the *xy*-plane for the energy density. After some straightforward algebra the SAM and OAM components have the form

$$S^A_{\zeta} = \frac{\hbar\int_0^{\infty}\left[\rho d\rho\left(J^2_{\ell-1}-J^2_{\ell+1}\right)/\left(\rho^2+\zeta^2\right)\right]}{\int_0^{\infty}\left[\rho d\rho\left(J^2_{\ell-1}+J^2_{\ell+1}\right)/\left(\rho^2+\zeta^2\right)\right]} \quad (4a)$$

$$L^A_{\zeta} = \frac{\hbar\int_0^{\infty}\left\{\rho d\rho\left[(\ell-1)J^2_{\ell-1}+(\ell+1)J^2_{\ell+1}\right]/\left(\rho^2+\zeta^2\right)\right\}}{\int_0^{\infty}\left[\rho d\rho\left(J^2_{\ell-1}+J^2_{\ell+1}\right)/\left(\rho^2+\zeta^2\right)\right]} \quad (4b)$$

With Eqs. (4a) and (4b), one can conclude that the TAM per photon of the APADs emitted CVV with topological charge ℓ is $J^A_{\zeta} = S^A_{\zeta} + L^A_{\zeta} = \ell\hbar$ within the paraxial limit. As to SAM, using the relation $\int_0^{\infty} xdxJ_n^2(x)/(x^2+a^2) = I_n(a)K_n(a)$ [10], where $I_n(a)$ and $K_n(a)$ are the first and second kind modified Bessel functions, respectively, and the asymptotic expansion for $I_n(a)K_n(a)$ (for example, Eq. (9.7.5) in [11]), Eq. (4a) becomes

$$S^A_{\zeta} = \frac{\ell/\nu^2 + 3\ell\left(1-4\ell^2\right)/8\nu^4 + \ldots}{1-\left(4\ell^2+3\right)/8\nu^2 + 3\left(16\ell^4+56\ell^2-15\right)/128\nu^4 - \ldots}\cdot\hbar \quad (5)$$

Note that for integer ℓ, $S^A_{\zeta} = 0$ only holds if $\ell = 0$, in which case E_{ρ} and E_{ζ} vanish, and the emitted beam is purely azimuthally polarized. However, $L^A_{\zeta} \neq \ell\hbar$ when $\ell \neq 0$. Take $\ell = 1$ as an example, for $\lambda = 1.55\mu m$ and $R = 3.9\mu m$ corresponding to one of the devices demonstrated in [1], $S^A_{\zeta} \approx 0.004\hbar$ and $L^A_{\zeta} \approx 0.996\hbar$. Such unwell-defined SAM and OAM is not surprising if one recalls that, as suggested by Eq. (2), the CVV can be decomposed into two scalar vortex beams, but not with constant weight. This Bessel-form superposition of two orthogonal scalar waves results in a hybrid mode, which is not the eigenmode of the paraxial wave equation and therefore does not have the SAM of $\pm\hbar$ per photon as the spin eigenstates of spin-1 particles usually do. Similar results can be derived for RPAD structures.

The AM carried by the APAD/RPADs emitted CVVs should also be investigated without invoking the paraxial approximation, such as for the case of small emitting structures ($R \ll \lambda$). However, it is well known that the identification of spin and orbital parts of optical AM beyond the paraxial limit is not straightforward and meets fundamental difficulties [12-14]. In 2002, Barnett demonstrated that it was the AM stored in an unit length, often taken as the AM 'flux', leading to the theoretical difficulty, and introduced the correct form of AM flux with the AM continuity equation [15]. The z component of the cycle-averaged AM flux through a plane oriented in the z-direction can be separated into physically meaningful spin and orbital parts, as [15]

$$M_{S,zz} = \frac{1}{2\mu_0\omega}\mathrm{Re}\left[-j\iint\rho d\varphi d\rho\left(E_x B_x^* + E_y B_y^*\right)\right] \quad (6a)$$

$$M_{L,zz} = \frac{1}{4\mu_0\omega}\mathrm{Re}\left[-j\iint\rho d\varphi d\rho\left(-\frac{B_x^*\partial E_y}{\partial\varphi} + \frac{E_y\partial B_x^*}{\partial\varphi} - \frac{E_x\partial B_y^*}{\partial\varphi} + \frac{B_y^*\partial E_x}{\partial\varphi}\right)\right] \quad (6b)$$

where ω is the angular frequency, and B_i ($i = x, y$) is the corresponding magnetic field. Besides, the SAM and OAM fluxes of a nonparaxial scalar vortex with a globally defined σ_z and topological charge of ℓ have the simple relation with the energy flux F, as $M_{S,zz}/F = \sigma_z/\omega$ and $M_{L,zz}/F = \ell/\omega$, respectively.

Here a numerical approach is used. First, instead of from the analytical expressions as Eqs. (1a)-(1c), the electric and magnetic fields are obtained by numerically calculating the far-field interference of the q-element APADs, and then Eqs. (6a) and (6b) are integrated numerically. The calculated ratio of the AM fluxes to energy flux as the function of topological charge is illustrated in Fig. 2, where q = 36, $R = 3.9\mu m$, $\lambda = 1.55\mu m$, and the ratio is presented as multiplied by ω. Returning to the aforementioned $\ell = 1$ case in which S_ζ^A was found nonzero in the paraxial limit, the numerically calculated nonparaxial fluxes are $(M_{S,\zeta\zeta}^A/F)\cdot\omega \approx 0.00396$ and $(M_{L,\zeta\zeta}^A/F)\cdot\omega \approx 0.996$. The SAM components (indicated by + marks in Fig. 2) for other ℓ values generally have nonzero values, and only equals to zero when $\ell = 0$. Although the TAM per photon of the APADs emitted CVV is perfectly defined as $\ell\hbar$ (x marks), its OAM component generally isn't (○ marks). A similar conclusion can also be drawn for RPADs emitted CVVs.

Additionally, one may notice that in Eq. (5), apart from the topological charge, S_ζ^A also varies with the normalized propagation constant $\nu = 2\pi R/\lambda$, or, with the radius of the angular-dipole structure for a certain wavelength. It is easy to prove that when $\nu \gg \ell$, which requires $R/\lambda \gg 1$, S_ζ^A tends to zero, and L_ζ^A approaches $\ell\hbar$. On the other hand, however, if the radius satisfies $R/\lambda \ll 1$, the APAD/RPADs emitted CVVs have relatively significant longitudinal components, and the paraxial approximation no longer holds. Neither does Eq. (5). Again by means of the numerical model for the APAD/RPADs far-field radiation, the SAM and OAM variations as a function of the normalized radius $R_n = R/\lambda$ is shown in Fig. 3, where $\lambda = 1.55\mu m$.

In fact, for $R_n \ll 1$, it is easy to find that the angular-dipole structure is equivalent to the extensively studied case of circularly polarized dipole radiation [15,16]. In [15], it is indicated that the flux ratio of AM to energy through a sphere, which is centered on the dipole of complex moment $\mathrm{P}_i \exp(-j\omega t)$ (i=x,y), is σ_z/ω, where $\sigma_z = j(\mathrm{P}_x\mathrm{P}_y^* - \mathrm{P}_y\mathrm{P}_x^*)$. Therefore, it is analogous in the $\ell = \pm 1$ case that when $R_n \ll 1$, the two dipoles of each dipole pair, ($\mathbf{P}_m^A$, $\mathbf{P}_{m+q/4}^A$) or ($\mathbf{P}_m^R$, $\mathbf{P}_{m+q/4}^R$), have the phase difference of $\ell(\phi_{m+q/4} - \phi_m) = \pm\frac{\pi}{2}$ and orthogonal polarizations ($\hat{\varphi}_m \cdot \hat{\varphi}_{m+q/4} = 0$, $\hat{\rho}_m \cdot \hat{\rho}_{m+q/4} = 0$), forming a beam with AM flux ratio of $\pm 1/\omega$. Consequently, all $q/2$ pairs of dipoles emit a beam of $M_{\zeta\zeta}^A/F = \pm 1/\omega$, or $M_{\zeta\zeta}^R/F = \pm 1/\omega$, constructively. Although it has not been suggested in [15] that this AM flux can be separated into spin and orbital components, as shown in Fig. 3(a) and 3(c), half of the AM flux is attributed to spin and the other half to orbital angular momentum. Interestingly, this agrees well with the analytical prediction in [16]. For $\ell = \pm 2$, the dipole elements on the opposite sides of the circumference tend to cancel each other when $R_n \ll 1$, and the AM flux only starts to emerge when $R_n \approx 1$, as shown in Fig. 3(b) and 3(d). In general, for odd orders of ℓ , the AM flux evolves from $M_{S,\zeta\zeta}/F = M_{L,\zeta\zeta}/F = \pm\frac{1}{2}/\omega$ when $R_n \ll 1$, while from $M_{S,\zeta\zeta}/F = M_{L,\zeta\zeta}/F = 0$ for even ℓ. It should also be noted that as the radius increases, there exists a critical radius for the APADs structure, where the spin component becomes unitary (1 for $\ell > 0$ and –1 for $\ell < 0$, see Fig. 3(a) and 3(b)) and the emitted beam is globally circular-polarized over the transverse plane. The reason of this difference between APADs and RPADs lies in the fact that APAD elements are linearly polarized along the azimuthal direction, in which the spinning of circular polarization is also defined. However, RPAD elements are polarized in the orthogonal direction of the polarization space, and it is not periodic in this dimension, which allows no complete spinning consequently.

On the other hand, when $R_n \gg 1$, the distance between the two dipoles of each pair $\sqrt{2}R \gg \lambda$, and the correlation between them vanishes (note the rapid variation in SAM and OAM when $R_n \approx 1$ in Fig. 3), resulting in the emergence of spatially helical phase front, as shown in Fig. 4. This diminishes the spin component and defines the orbital angular momentum as $\ell\hbar$ per photon. In general, the increase in R leads to spin-to-orbit AM conversion, by radially 'decentralizing' the linear polarization components of the spinning light field. In other words, if the linear components of spinning light source are detached in a geometrically significant distance ($R \gg \lambda$) from each other, the intrinsic phase delay between them is reconstructed into the geometric phase in the polarization state space, or, Pancharatnam phase [17], which has been shown to account for the OAM carried by cylindrical vector beams [18].

In conclusion, we investigate the angular momentum carried by a general class of cylindrical vector vortices, typically generated by optical vortex emitters with cylindrically symmetric emission structures. By calculating the AM components of the angular-dipoles emitted CVVs, it can be concluded that these optical vortex emitters, with practical dimensions ($R > \lambda$), are shown to emit well-defined TAM of $\ell\hbar$ per photon. Moreover, it has also been shown that the OAM/SAM ratio is dependent on the emitter size, indicating a dynamic conversion between the two mechanically equivalent counterparts. It is further revealed that, as emitter dimension increases, the intrinsic SAM carried by the cylindrically rotating SOP of the dipole collection is gradually converted into OAM, resulting in practically pure and well-defined OAM emitter. These results clarify the common misconception of the OAM states carried by CVVs, and provide useful instructions for techniques of the optical vortex generation.

Acknowledgement

S. Yu and X. Cai are grateful to Prof. Sir Michael Berry for useful discussions. The project is partially funded by the Chinese Ministry of Science and Technology under project 2014CB340000. J. Zhu's research at University of Bristol is funded by the China Scholarship Council (201306100054).

References

1. X. Cai, J. Wang, M. J. Strain, B. Johnson-Morris, J. Zhu, M. Sorel, J. L. O'Brien, M. G. Thompson, and S. Yu, Science **338**, 363 (2012).
2. N. K. Fontaine, C. R. Doerr, and L. Buhl, OSA Technical Digest (Optical Society of America, Washington, DC, 2012), paper OTu11.2.
3. Z. Zhao, J. Wang, S. Li, and A. E. Willner, Opt. Lett. **38**, 932 (2013).
4. L. Allen, M. Beijersbergen, R. Spreeuw, and J. Woerdman, Phys. Rev. A **45**, 8185 (1992).
5. J. Zhu, X. Cai, Y. Chen, and S.Yu, Opt. Lett. **38**, 1343 (2013).
6. W. Nasalski, Opt. Lett. **38**, 809 (2013).
7. W. Nasalski, Appl. Phys. B **115**, 155 (2014).
8. V. N. Belyi, N. A. Khilo, S. N. Kurilkina and N. S. Kazak, J. Opt. **15**, 044018 (2013).
9. M. V. Berry, Proc. SPIE **3487**, 6 (1998).
10. I. S. Gradshteyn and I. M. Ryzhik, *Table of Integrals, Series, and Products, Seventh Edition* (Academic, New York, 2006).
11. M. Abramowitz and I. A. Stegun, *Handbook of mathematical functions* (Dover, New York, 1965).
12. S. M. Barnett and L. Allen, Opt. Commun. **110**, 670 (1994).
13. S. van Enk and G. Nienhuis, Europhys. Lett. **25**, 497 (1994).
14. S. M. Barnett, J. Mod. Opt. **57**, 1339 (2010).
15. S. M. Barnett, J. Opt. B: Quantum Semiclass. Opt. **4**, S7 (2002).
16. J. H. Crichton and P. L. Marston, Electron. J. Diff. Eqns. Conf. **04**, 37 (2000).
17. S. Pancharatnam, Proc. Indian Acad. Sci. A **44**, 247 (1956).
18. Z. Bomzon, G. Biener, V. Kliener, and E. Hasman, Opt. Lett. **27**, 285 (2002).

Figures

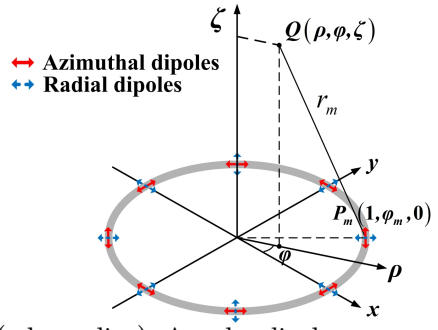

Fig. 1 (color online). Angular-dipole groups as the basic constructing elements of the CVV emitters: APADs (red solid arrows) and RPADs (blue dashed arrows).

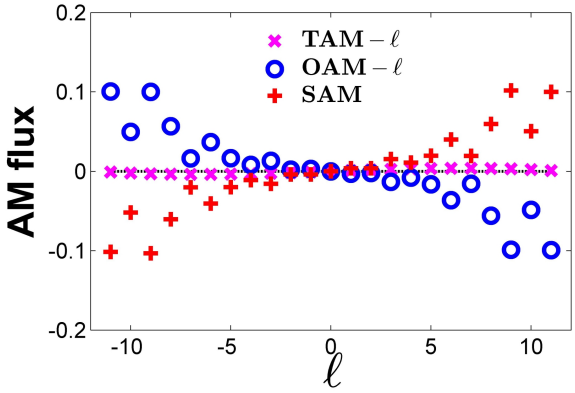

Fig. 2 (color online). Numerically calculated ratio of the far-field AM fluxes to energy flux of CVVs emitted by an APAD group, as a function of topological charge. q = 36, $R = 3.9\mu m$, and $\lambda = 1.55\mu m$. The ratios of the TAM fluxes (×) and the OAM flux (○) to the energy flux are presented as the difference between the ratios and the topological charge; the spin components are illustrated by the + marks.

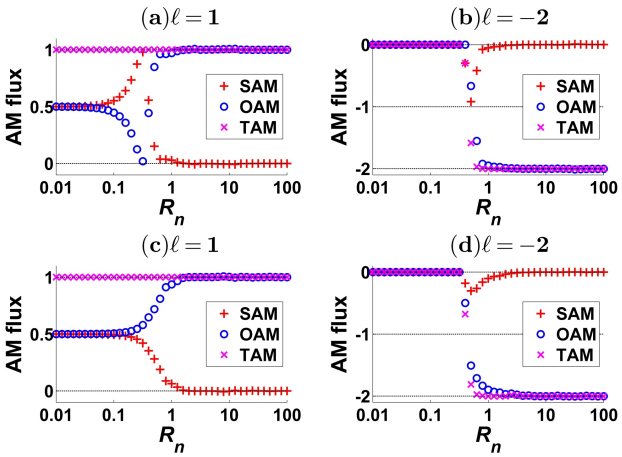

Fig. 3 (color online). Numerically calculated ratios of the AM fluxes to energy flux of the angular-dipoles emitted CVVs. The spin (+), orbital (○) components and total angular momentum flux (×) as a function of the normalized radius ($\lambda = 1.55\mu m$) are illustrated as (a) APADs, $\ell = 1$, (b) APADs, $\ell = -2$, (c) RPADs, $\ell = 1$, and (d) RPADs, $\ell = -2$.

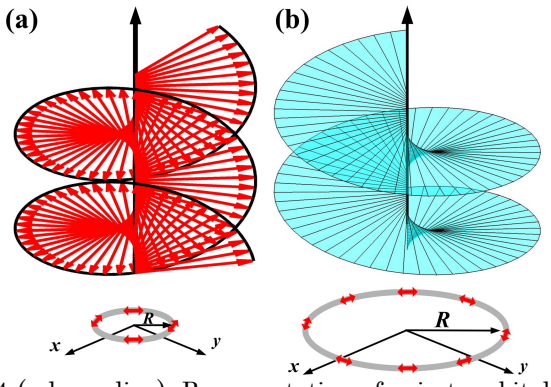

Fig. 4 (color online). Representation of spin-to-orbital AM conversion of APADs emitted beam when $\ell = 1$: from (a) circularly polarized beam when at the critical radius, to (b) vectorial vortex beam with well-defined OAM when $R_n \gg 1$.

Full citation listings:

1. X. Cai, J. Wang, M. J. Strain, B. Johnson-Morris, J. Zhu, M. Sorel, J. L. O'Brien, M. G. Thompson, and S. Yu, *Integrated Compact Optical Vortex Beam Emitters*, Science **338**, 363 (2012).
2. N. K. Fontaine, C. R. Doerr, and L. Buhl, *Efficient Multiplexing and Demultiplexing of Free-space Orbital Angular Momentum Using Photonic Integrated Circuits*, in *Optical Fiber Communication Conference, OSA Technical Digest* (Optical Society of America, Washington, DC, 2012), paper OTu1l.2.
3. Z. Zhao, J. Wang, S. Li, and A. E. Willner, *Metamaterials-based Broadband Generation of Orbital Angular Momentum Carrying Vector Beams*, Opt. Lett. **38**, 932 (2013).
4. L. Allen, M. Beijersbergen, R. Spreeuw, and J. Woerdman, *Orbital Angular Momentum of Light and the Transformation of Laguerre-Gaussian Laser Modes*, Phys. Rev. A **45**, 8185 (1992).
5. J. Zhu, X. Cai, Y. Chen, and S.Yu, *Theoretical Model for Angular Grating-based Integrated Optical Vortex Beam Emitters*, Opt. Lett. **38**, 1343 (2013).
6. W. Nasalski, *Exact Elegant Laguerre-Gaussian Vector Wave Packets*, Opt. Lett. **38**, 809 (2013).
7. W. Nasalski, *Vortex and Anti-vortex Compositions of Exact Elegant Laguerre-Gaussian Vector Beams*, Appl. Phys. B **115**, 155 (2014).
8. V. N. Belyi, N. A. Khilo, S. N. Kurilkina and N. S. Kazak, *Spin-to-orbital Angular Momentum conversion for Bessel Beams Propagating Along the Optical Axes of Homogeneous Uniaxial and Biaxial Crystals*, J. Opt. **15**, 044018 (2013).
9. M. V. Berry, *Paraxial Beams of Spinning Light*, Proc. SPIE **3487**, 6 (1998).
10. I. S. Gradshteyn and I. M. Ryzhik, *Table of Integrals, Series, and Products, Seventh Edition* (Academic, New York, 2006).
11. M. Abramowitz and I. A. Stegun, *Handbook of mathematical functions* (Dover, New York, 1965).
12. S. M. Barnett and L. Allen, *Orbital Angular Momentum and Nonparaxial Light Beams*, Opt. Commun. **110**, 670 (1994).
13. S. van Enk and G. Nienhuis, *Spin and Orbital Angular Momentum of Photons*, Europhys. Lett. **25**, 497 (1994).
14. S. M. Barnett, *Rotation of Electromagnetic Fields and the Nature of Optical Angular Momentum*, J. Mod. Opt. **57**, 1339 (2010).
15. S. M. Barnett, *Optical Angular-momentum Flux*, J. Opt. B: Quantum Semiclass. Opt. **4**, S7 (2002).
16. J. H. Crichton and P. L. Marston, *The Measurable Distinction Between the Spin and Orbital Angular Momentum of Electromagnetic Radiation*, Electron. J. Diff. Eqns. Conf. **04**, 37 (2000).
17. S. Pancharatnam, *Generalized Theory of Interference, and Its Applications*, Proc. Indian Acad. Sci. A **44**, 247 (1956).
18. Z. Bomzon, G. Biener, V. Kliener, and E. Hasman, *Radially and Azimuthally Polarized Beams Generated by Space-variant Dielectric Subwavelength Gratings*, Opt. Lett. **27**, 285 (2002).